Cationic poly(cyclodextrin)/alginate nanocapsules: From design to application as efficient delivery vehicle of 4-hydroxy tamoxifen to podocyte in vitro

Sabrina Belbekhouche, Julie Oniszczuk, André Pawlak, Imane El Joukhar, Angélique Goffin, Gilles Varrault, Dil Sahali, Benjamin Carbonnier

Cationic Poly(cyclodextrin)/Alginate Nanocapsules: From Design to Application as Efficient Delivery Vehicle of 4-hydroxy tamoxifen to Podocyte *in vitro*

Sabrina Belbekhouche,[1*] Julie Oniszczuk,[2] André Pawlak, [2] Imane El Joukhar, [1] Angélique Goffin, [3] Gilles Varrault, [3] Dil Sahali, [2] Benjamin Carbonnier[1**]

1- Université Paris Est, ICMPE (UMR 7182), CNRS, UPEC, F-94320 Thiais, France
2- INSERM U955, Equipe 21, Centre de Référence Syndrome Néphrotique Idiopathique UPEC Créteil France
3- LEESU, Université Paris-Est (UMR MA 102), Ecole des Ponts ParisTech, UPEC, AgroParisTech, Créteil, France

* and ** authors for correspondence :

* Dr Sabrina Belbekhouche
Université Paris Est, ICMPE (UMR 7182), CNRS, UPEC, F-94320 Thiais, France
belbekhouche@icmpe.cnrs.fr, phone: + 331 4978 1149, fax: + 331 4978 1208

** Prof Dr Benjamin Carbonnier
Université Paris Est, ICMPE (UMR 7182), CNRS, UPEC, F-94320 Thiais, France
carbonnier@icmpe.cnrs.fr, phone: + 331 4978 1114, fax: + 331 4978 1208.

Total numbers of words: 4,477 words, 8 figures in manuscript

Abstract. (173 words)

Most of the drug molecules are partially insoluble in aqueous solution and then may accumulate in fat tissues hampering efficient therapy. Innovative drug delivery strategies have emerged in industry or academia over the last decades, however preserving the activity of the encapsulated drug, having high drug loading capacity and controlling drug release kinetics are still challenging. In this context, we explored the preparation of new nanocarriers, namely nanocapsules, *via* a templating method, and using polysaccharides exhibiting biological functions. Cationic poly(cyclodextrin) ($P(CD^+)$) and alginate (alg^-) were initially self-assembled layer-by-layer on colloidal gold nanoparticles. Removal of gold nanoparticles was then induced thorough cyanide-assisted hydrolysis, enabling the recovery of nanocapsules. A hydrophobic drug known to allow the mutation of genes inside cells, namely 4-hydroxy-tamoxifen, was loaded within the nanocapsules' shell via inclusion with the cyclodextrin cavities. The so-designed nanomaterials were incubated with immortalized podocytes to investigate *i*) their incorporation inside cells and *ii*) their efficiency for *in vitro* 4-hydroxy-tamoxifen-induced CreERT2 recombination. This work undoubtedly highlights a proof-of-concept for drug delivery using polysaccharides-based capsules with host properties.

Keywords: particle-templated layer-by-layer assembly, poly(cyclodextrin), capsule, supramolecular chemistry, host−guest complexation, podocyte

1. Introduction.

Nowadays, the efficient delivery of hydrophobic drugs is still a key challenge in the field of biotechnology.[1, 2] The limited clinical effectiveness may result from low solubility in aqueous media, toxicity profile, and/or other poor pharmaceutical characteristics. The development of drug vehicles has then been considered for encapsulating and delivering poorly water-soluble drugs for several therapies. [3]. For the design of polymer-based delivery systems various types of carrier-drug interactions, including electrostatic or host–guest ones, may be considered providing innovative solutions for carrying one or multiple drug payloads. Similarly to common host molecules such as pillararenes, cucurbiturils and crown ethers, low toxic cyclic oligosaccharides as cyclodextrins (CDs) can incorporate various guest molecules into their hydrophobic cavity, thereby enabling enhanced solubilization of high amounts of hydrophobic drugs and potentially transport though cell membranes.[4]

In the literature, two strategies are presented to prepare CD-containing LbL assemblies. The first one involves the use of charged CDs, and the LbL assemblies are obtained through electrostatic interactions. [5-7] Nevertheless, molecular cyclodextrins did not provide highly stable entrapment of the guest molecules, leading to a rapid drug release. The second strategy for constructing CD-containing LbL assemblies relies on the use of host–guest complexation as the driving force for the assembly built up.[8-11] In this case, CD-containing polymers and guest molecule-appended polymers are built into LbL multilayers by forming host–guest complexes.

Herein we propose an alternative path based on supramolecular chemistry for both the self-assembly of multilayered nanocapsules and the encapsulation of 4-hydroxytamoxifen *via* electrostatic and hydrophobic effect driven inclusion complex formation, respectively. The as-designed nanometer-sized hollow polymeric spheres (or capsules) are expected to exhibit high stability over a wide pH range, and enable efficient intracellular drug delivery. LbL-based hollow capsules are generally stable, explaining the interest of using them as drug carriers. [12, 13] Indeed, our approach involves the use of a charged polymeric carrier, namely a cationic polycyclodextrin, capable of complexation with a hydrophobic chemical in alternation with a degradable polyanion (the alginate). The synthesis of the polycation was previously reported [14] but no previous study explored its potential use for the elaboration of capsules with drug loading ability. Herein, the affinity of the cyclodextrin cavities has been

investigated with a model hydrophobic probe and a drug, namely pyrene and 4-hydroxy-tamoxifen (OHT), respectively. [15]

OHT is the major active metabolite of tamoxifen which binds selectively estrogen receptor (ER) and estrogen-related receptors (ERR) with estrogenic and anti-estrogenic effects. Physiopathologic systems have been investigated through transgenic tools implying the targeted expression of the Cre-recombinase fused with a mutated form of the ER. This latter allows high affinity binding of OHT and a low affinity for endogenous estrogen [15, 16]. The fusion protein translocates from the cytoplasm to the nucleus upon its binding with OHT. This involves the excision of genomic segments between loxP sequences.

In our study, we will use a conditionally immortalized mouse podocytes cell line which has been developed from transgenic mice Cmip conditional knock-out mice as described elsewhere [17]. Indeed, these mice possess coding sequences for the chimeric Cre recombinase associated with the mutated domain of the estrogen receptor (CreERT2). Upon treated with binding OHT, the chimeric CreER protein translocation in the nucleus is induced where the recombinase can play its role and thus cause the deletion of the exon 8 of the second allele. It deserves noting that the formation the inclusion complex between tamoxifen and its derivatives and CD has already been reported [18, 19] but to the best of our knowledge, there are no studies reporting the host–guest (polycationic CD–4-hydroxytamoxifen) interaction-mediated Cmip exon 8 deletion in podocytes selected as an *in vitro* model. Thus, this contribution aims at providing evidences for (*i*) the efficient loading of 4-hydroxytamoxifen within polycationic CD-alginate multilayered nanocapsules through inclusion complex formation, (*ii*) the preservation of the biological activity of OHT through such delivery pathway.

2. Experimental section

2.1. Materials

The following chemicals were used as received: chitosan (chi^+, Sigma-aldrich), alginate (alg^-, Sigma-aldrich), sodium 2-mercaptoethanesulfonate (Sigma-aldrich, > 89.5%), pyrene (Sigma-Aldrich), 4-hydroxy-tamoxifen (OHT, Sigma-Aldrich), gold nanoparticles (60 nm, Sigma-Aldrich) and potassium cyanide (KCN, Sigma-Aldrich). The cationic cyclodextrin ($P(CD^+)$) was synthesized according to the procedure developed by Thuaud et coll. [14] ~~The cationic cyclodextrin polymer was synthesized by crosslinking the β-cyclodextrin (β-CD) with epichlorohydrin [20] followed by a reaction with the 2,3-epoxypropyltrimethylammonium~~

~~chloride.[14] Briefly, β-CD reacted in NaOH solution (33 %) with epichlorohydrin at 50 °C for 210 min. After neutralizing the pH, the polymer was concentrated by ultrafiltration to remove salt or low molecular compounds and recovered through freeze drying process. The resulting β-CD polymer was chemically modified with quaternary ammonium side groups through reaction with 2,3-epoxypropyltrimethylammonium chloride in basic media. The resulting modified polymer was purified by a dialysis step using a cellulose dialysis membrane (1 kDa cut-off). The product was isolated via freeze drying to yield a white solid.~~ Average molar masses and molar masses distributions were determined by size exclusion chromatography (SEC) coupled online with multi-angle light scattering (MALS) and differential refractive index (DRI) detectors. The MALS apparatus is the DAWN Heleos-II from Wyatt Technology (Ca, USA) filled with a K5 cell and a Ga–As laser (λ= 690 nm). The DRI detector is a Shimadzu RID-10A (Japan). Columns [Shodex SB OHpak 804 and 806 HQ for alginate (dn/dc = 0.140 mL.g^{-1} [21]) and PL aquagel OH 40+30 for the cationic polycyclodextrin] were eluted with 0.1mol.L^{-1} $LiNO_3$ at 0.5 mL min^{-1}. The flow rate was fixed at 1 mL.min^{-1}. The samples were filtered on 0.45 µm unit filter before injection through a 100 µL full loop.

For the alginate, the $\overline{Mn}$ value is 2.7 10^5 g·mol^{-1}, the $\overline{Mw}$ value is 3.8 10^5 g·mol^{-1}. ~~For the cationic poly(cyclodextrin), the $\overline{Mn}$ value is 6.5 10^3 g·mol^{-1}, the $\overline{Mw}$ value is 2.4 10^4 g·mol^{-1} and the degree of substitution is 0.40 ±0.05 (estimated from ^{1}H NMR [14]).~~

2.2. Synthetic procedures

2.2.1. Elaboration of P(CD$^+$)/alginate multilayers films onto flat gold substrate

A Q-Sense E1 device (Q-Sense, Sweden) was employed to monitor the *in situ* formation of the multilayer self-assembly of (P(CD$^+$)/alg$^-$) bilayers. The gold coated QCM crystals were first cleaned with water and ethanol, then treated in an UV/ozone chamber (BioForce UV/Ozone ProCleaner) for 20 min and pretreated with sulfonated thiol (5 g.L^{-1}, 10 mg sodium 2-mercaptoethanesulfonate in 2 mL of water). This sulfonated thiol derivative is used as an anchoring layer for enabling the further adsorption of the polycation layer. After a supplementary rinsing with ethanol, surfaces were dried under N_2 flow. After mounting in the QCM-D flow chamber, the sensor was conditioned in water for 10 min prior to monitoring the self-assembly. All solutions were injected into the cell with a flow rate of 250 µL.min^{-1} at 25 °C. The self-assembly of P(CD)$^+$ / alg$^-$ was performed onto the pretreated negatively charged flat gold substrate via alternative contact with first the polycation followed by the polyanion

solutions. Wetting angle measurements were performed at room temperature with a Krüss apparatus in the sessile drop configuration. A drop (5 µL) was laid upon a flat gold substrate bare or modified with the multilayer film, and then, an image was captured using a black and white CCD camera.

2.2.2 Fabrication of P(CD$^+$)-based nanocapsules

In order to adsorb the cationic-poly(cyclodextrin) and the polyanionic alginate on the spherical surface, the colloidal gold nanoparticles were first pretreated with a thiol derivative (sulfonate groups on the surface). 500 µL of a filtered suspension of gold nanoparticles, 400 µL of aqueous solution and 100 µL of sodium 2-mercaptoethanesulfonate solution (5 g.L^{-1}, 10 mg in 2 mL of water) were mixed overnight in an Eppendorf tube. Free thiol derivative was removed from the supernatant after centrifugation (17968 g for 15 min). 100 µL of cationic-poly(cyclodextrin) (1 g.L^{-1} prepared in water) solution was added to a suspension of pre-treated gold nanoparticles. After 20 min, the polyelectrolyte excess was removed from the supernatant fraction after centrifugation (17968 g for 15 min). This washing process was repeated two more times keeping the final volume equal to 1 ml. This adsorption process was further repeated with the addition of 100 µL of alginate solution (1 g.L^{-1} prepared in water) to the suspension of cationic-poly(cyclodextrin)-modified gold nanoparticles. This procedure describes the assembly of a single bilayer: (cationic-poly(cyclodextrin) /alginate)$_1$ (P(CD$^+$)/alg$^-$)$_1$. The LbL process was repeated to get the nanomaterials with a desired number of layers. This process was monitored with zeta potential measurement (Zetasizer Nano-ZS, Malvern Instrument).

Nanocapsules were obtained by dissolving the gold core using 100 µL of potassium cyanide solution (70 mg of KCN in 15 mL of water). This step was followed by a dialysis process to remove the gold complex (3.5 kDa cut off). Kinetic of the core removal was investigated through monitoring the spectroscopic signature of the gold core. Absorbance spectra were recorded with a UV-Visible spectrophotometer from Varian Cary 50 Bio. Non presence of gold complex was investigated in the last dialysat and in capsules by the Inductively Coupled Plasma Optical Emission Spectrometry (ICP-OES) analyses (Au wt. %) (ICP-OES spectrometer, Simultaneous Varian Vista Axial). The capsules were viewed with transmission electron microscopy (TEM), a droplet of nanomaterial suspension and one of a solution of uranyle acetate (0.7 wt %) were deposited on a plasma pre-treated copper TEM grid and allowed to dry in air at room temperature prior analysing. Transmission Electron Microscopy

(TEM) were conducted on a Tecnai F20 ST microscope (field-emission gun operated at 3.8 kV extraction voltage) operating at an acceleration voltage of 200 kV.

2.3. **Loading of hydrophobic chemicals inside CD cavity**

Hydrophobic chemicals (pyrene and 4-hydroxy-tamoxifen) were loaded inside the cyclodextrin cavity.

The pyrene entrapment was achieved through simple diffusion process of this molecule from solution through P(CD^+)-based multilayer films preassembled on pretreated gold substrates, namely flat surface (QCM sensor crystal) and nanoparticles. In the former case, gold coated QCM Sensor Crystal was initially modified with an anchoring sulfonate thiol layer and ($P(CD^+)/alg^-)_4$-P(CD^+) LbL films under dynamic flowing of the corresponding solutions in the QCM cell. Polyelectrolytes-coated quartz slides were flushed with the pyrene solution (4.10^{-7} $mol.L^{-1}$)

P(CD^+)-based nanocapsules was overnight incubated with 50 µL pyrene solution (4.10^{-7} $mol.L^{-1}$, preparation described below) or a 4-hydroxy-tamoxifen solution (1 ~~µM~~ µmol.L^{-1} prepared in ethanol).

Preparation of a pyrene solution at 4.10^{-7} $mol.L^{-1}$: A stock solution of pyrene (10^{-3} mol L^{-1}) was prepared in acetone. 200 µL aliquot of this solution was introduced into empty flask and the solvent was evaporated. After evaporation, the flask were filled with 500 mL of water and gently stirred for 24 h. The final pyrene concentration was 4.10^{-7} $mol.L^{-1}$. All samples were excited at 332 nm and the emission spectra of pyrene showed five vibronic peaks notably at 372 nm and 382 nm. The ratios I_{372}/I_{382} (error less than 5%) were then calculated leading to a measure of the polarity of the pyrene micro-environment.[22] Fluorescence measurements were performed with a spectrofluorimeter (Japan, Jasco) equipped with a xenon lamp. The amount of pyrene incorporated in the CD cavity was estimated by fluorescence intensity measurements after the extraction of pyrene from capsules with methanol. The suspension of capsules (100 µl, 950 million nanoparticles) was centrifuged, and the supernatant was removed. The experiment was performed with pyrene-loaded ($P(CD^+)/alg^-)_n$-P(CD^+)-coated (n = 2 and 4) particles. After the addition of methanol (500 µL), the suspension was again centrifuged, and the supernatant containing pyrene was recovered. This process was repeated

two times to ensure the total extraction of pyrene from the capsules. Then, the fluorescence intensity of the solutions was measured.

2.4. In Vitro Biocompatibility Studies.

Cell Culture. Immortalized mouse podocytes were cultured under permissive conditions: RPMI 1640 medium containing 10% fetal calf serum, penicillin (100 µg/ml), streptomycin (100 µg/ml), 1% of non-essential amino acids, 1% of HEPES, 1% of sodium pyruvate and interferon-γ (IFN-γ, 50 U/ml), at 33°C. At 60-80% confluence on 6-well plates, the 4-hydroxy-tamoxifen-loaded nanomaterials (x 9.5 10^9 particles/ml) were immediately added to the cells. After exposure to nanoparticles for 48h, cells were harvested and genotyping was processed afterwards

Genotyping. Podocytes were washed 3 times with 1X PBS solution and then suspended in lysis buffer (0.1 M Tris pH 8, 0.2 M NaCl, 0.2 % SDS, 5 mM EDTA, 150 µg/ml proteinase K). After incubation at 55°C and complete lysis of the sample, the DNA was purified by the phenol/chloroform extraction technique and then precipitated with ethanol. The resulting genomic DNA pellet was dissolved in water and the DNA concentration was measured by nanodrop. This solution was then diluted to a concentration of 150 ng/ml. 2 µl of this solution are used for the PCR reaction. The PCR conditions were as follows: step 1 : 95 °C for 5 minutes ; step2 : 95°C for 30 seconds ; step 3 : 60°C for 30 seconds ; step 4 : 72 °C for 90 seconds) and then repeat steps 2–4 for 30 cycles then finally keep at 72°C for 10 min. the PCR primer forward and reverse are respectively : Cmip lox Forward : ACACTGGAGTCTCTCTCACTGCTGGC; Cmip lox Reverse : GAGAACATCTGAAAAGGACACAGGCC

After the PCR, the samples migrate on a 1.2% agarose gel, in a migration buffer (Tris-base, boric acid, EDTA and H_2O). The expected size of the fragments with the Cmip allele is 976 bp (Cmip lox).

The following conditions have been tested on these podocytes with two controls. The first one consists in cells, untreated with nanoparticles (negative control), the second consists in cells treated with 2 layers 4-hydroxy-tamoxifen-loaded $(P(CD^+)/alg^-)_n$-$P(CD^+)$ particles with gold core. The third condition consists in cells treated 2 layers 4-hydroxy-tamoxifen-loaded $(P(CD^+)/alg^-)_n$-$P(CD^+)$ particles without gold core. 475 million nanoparticles (50 µl) are

injected into each well. Finally the last condition consists in cells treated with 10 µl of a 4-hydroxy-tamoxifen solution (1 ~~µM~~ µmol.L^{-1} prepared in ethanol).

3. Results and discussion

Polymeric nanoparticles/assemblies are promising candidates for oral drug delivery of hydrophobic drugs by virtue of their potential biocompatibility and biodegradability especially when using polysaccharides, ability to increase drug solubility and to shield the entrapped drug from external harsh conditions of chemical or enzymatic degradation, for instances. To elaborate capsules able to selectively entrapped hydrophobic molecules inside the particle shell, a cationic poly(cyclodextrin) was layer-by-layer assembled with alginate onto a sacrificial gold template as outlined in Figures 1 and 2. Lastly, the template is selectively removed through gold hydrolysis and diffusion of the resulting water-soluble salts through the polyelectrolyte shell to ensure the capsules formation.

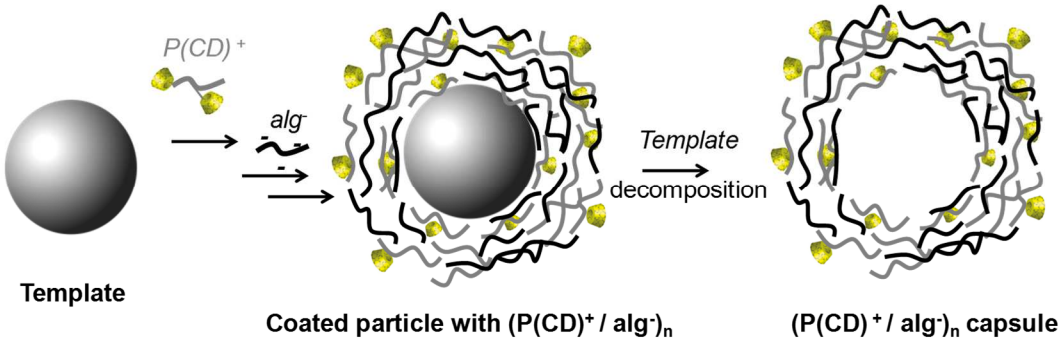

Figure 1: Schematic illustration of the polyelectrolyte adsorption process for the elaboration of cationic-poly(cyclodextrin) (P(CD$^+$)) /alginate (alg$^-$) capsules.

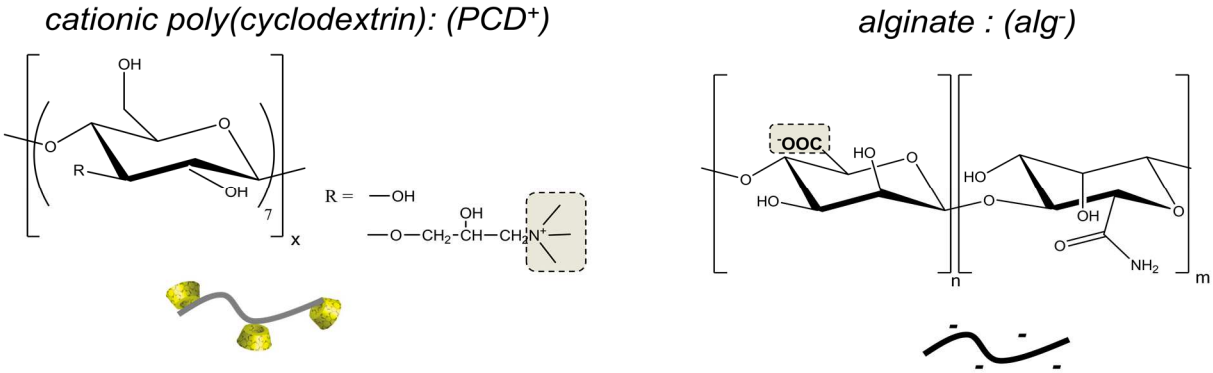

Figure 2: Chemical structure of the cationic poly(β-cyclodextrin) (x" symbolises an integer number representing the degree of polymerization) *and the polyanionic alginate.*

3.1. Elaboration of the cationic poly(β-cyclodextrin)

The cationic cyclodextrin polymer was synthesized by crosslinking the β-cyclodextrin (β-CD) with epichlorohydrin [20] followed by a reaction with the 2,3 epoxypropyltrimethylammonium chloride.[14] Briefly, β-CD reacted in NaOH solution (33 %) with epichlorohydrin at 50 °C for 210 min. After neutralizing the pH, the polymer was concentrated by ultrafiltration to remove salt or low molecular compounds and recovered through freeze-drying process. This results in a β-CD polymer containing dihydroxypropyl groups as substituents and hydroxypropyl groups as bridges linking β –CD. This polymer was then chemically modified with quaternary ammonium side groups through reaction with 2,3-epoxypropyltrimethylammonium chloride in basic media. The supposed structure is illustrated in Figure S1.The resulting modified polymer was purified by a dialysis step using a cellulose dialysis membrane (1 kDa cut off). The product was isolated via freeze-drying to yield a white solid.

For the cationic poly(cyclodextrin), the $\overline{Mn}$ value is 6.5 10^3 g·mol^{-1}, the $\overline{Mw}$ value is 2.4 10^4 g·mol^{-1} and the degree of substitution is 0.40 ±0.05 (estimated from ^{1}H NMR [14]).

3.2.~~1.~~ Proof of concept: Elaboration of the multilayer films onto flat gold substrate.

To confirm the success of the multilayer film elaboration, static contact angle measurements are performed on flat gold surfaces before and after deposition of the polyelectrolytes (Figure 3). The contact angle decreases from ~50° for a gold substrate pre-treated with the sulfonated thiol derivative (data not shown) to ~20° upon the layer-by-layer deposition process, in agreement with the hydrophilic nature of the adsorbed polysaccharides. This variation in wettability after the multilayer build-up is found to be independent of the number of layers.

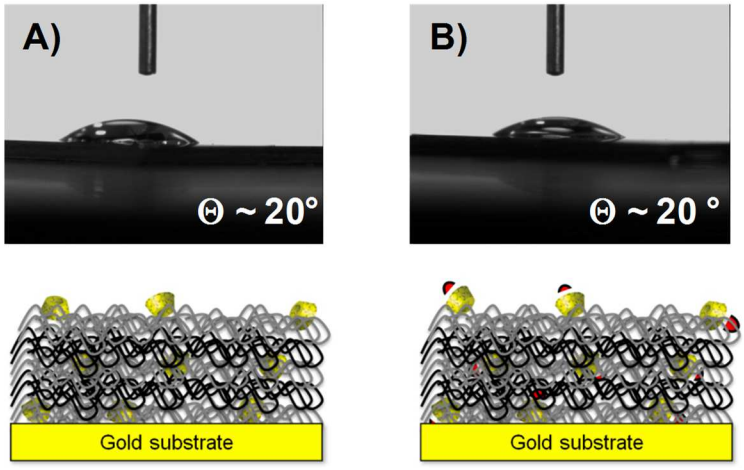

Figure 3: Water contact angle measurements on flat gold substrates A) after coating with $(P(CD^+)/alg^-)_4$-$P(CD^+)$ and B) after coating with pyrene-loaded$(P(CD^+)/alg^-)_4$-$P(CD^+)$.

The assembly of $P(CD)^+$ and alg^- in multilayer films was monitored by QCM-D measurements (Figure 4). A stable baseline is first measured prior to adsorption of the polyelectrolytes. After 10 minutes, a solution of $P(CD^+)$ (1 $mg.mL^{-1}$) is injected into the measurement chamber of the QCM-D. A decrease in frequency is then observed corresponding to the adsorption of the cationic $P(CD^+)$ to the sulfonated anionic gold substrate. $P(CD^+)$ is allowed to adsorb for 900 s before the rinsing step begins. It is assumed that this adsorption time enables sufficient surface coverage of sulfonated gold substrate with $P(CD^+)$ to lead to charge reversal of the interfacial layer that is a prerequisite for further polyanion adsorption. Upon rinsing, a slight increase in the frequency shift assigned to the polyelectrolyte excess removal is observed. It must be kept in mind that for the studied films the frequency changes as observed during the rinsing process are much smaller than those measured during the adsorption steps. The polyanionic alginate (1 $mg.mL^{-1}$) is then injected. A decrease in the resonance frequency is observed due to the adsorption of the anionic alginate macromolecules to the cationic polycyclodextrin adsorbed layer. Once again, free polyelectrolyte chains are removed during the rinsing step before the multilayer assembly was continually built up with consecutive adsorption of $P(CD^+)$ and alg^-. Typical decrease in the frequency signal by further increasing the number of adsorption cycles is then observed, indicating that mass was being added onto the surface. This is in agreement with previously reported results indicating that the adsorption of polyelectrolytes onto oppositely charged surfaces essentially leads to irreversible adsorbed layers in a predetermined range of pH, temperature, ionic strength.[13]

Further information may be obtained from dissipation monitoring about the viscoelastic properties of the polyelectrolyte multilayer films. The voltage imposed to the QCM is suspended and the decay of the amplitude of the crystal is measured as a function of time. From this, the dissipation factor *D*, is defined according to the following equation:

$$D = \frac{E_{dissipated}}{2\pi E_{stored}}$$

$E_{dissipated}$ and E_{stored} correspond to the dissipated energy and the stored energy respectively. A positive shift of *D* is typical assigned to less rigid (water-rich) structures.

Figure 4 shows the stepwise change in dissipation as the multilayer film is built up upon successive adsorption of P(CD^+) and alginate. The magnitude of the dissipation factor (dissipated energy) increases as a function of the bilayer number. For both polyelectrolytes, an initial rise in the dissipation is observed after flushing with polymer solution. The dissipation factor levels off rapidly yielding a plateau regime. Such behaviour suggests that upon adsorption of the polyelectrolyte layers, water molecules are coupled to the adsorbed polymer layers as an additional mass. The P(CD^+)/alg^- films can then be regarded as composed of polymer chains and entrapped water with viscoelastic characteristics.

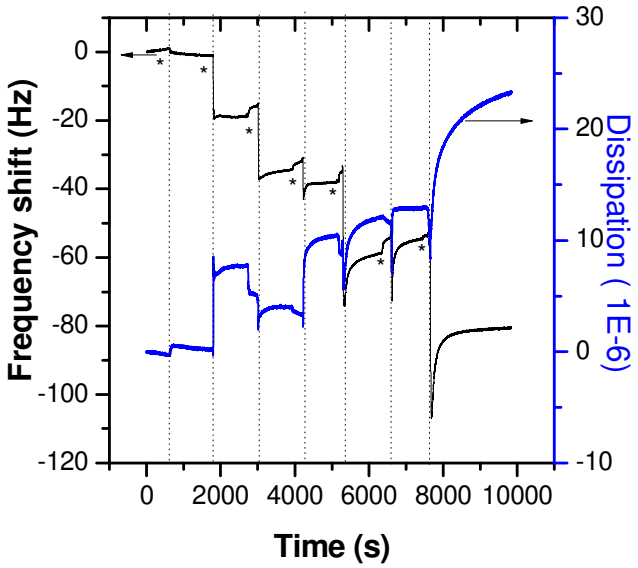

Figure 4: Monitoring of the LbL build-up of the $(P(CD^+)/alg^-)_n$ film on gold flat substrate by QCM-D experiment. The quartz crystal was initially placed in contact with solvent (noted ""); after an equilibrium time of 10 min, cationic poly(cyclodextrin) ($P(CD^+)$) and alginate (alg^-) solutions (1 mg.mL $^{-1}$) were alternatively added. A rinsing step was performed between each polymer deposition step.*

After elaboration of the $(P(CD^+)/alg^-)_4$ $P(CD^+)$ multilayer film, flushing the multilayer assembly with a solution of pyrene (4.10^{-7} mol.L^{-1} prepared in water) leads to a decrease of the equilibrium frequency shift of 10 ± 2 Hz. This evidences an increase of the film weight and then suggests an entrapment of pyrene through the multilayer film. It is worth mentioning that no variation in the equilibrium frequency shift is seen for the $(chi^+/alg^-)_4$ chi^+ multilayer film upon contact with the pyrene solution suggesting that the entrapment of pyrene within $(P(CD^+)/alg^-)_4$ $P(CD^+)$ results from inclusion complex formation. The water contact angle

value is around 20° (figure 3b) for the pyrene incubated with $(P(CD^+)/alginate)_4$-$P(CD^+)$ multilayer film.

Note that after elaboration of the multilayer film ($(P(CD^+)/alg^-)_4$ $P(CD^+)$), the latter has been flushed with culture medium. This film is stable as evidenced by QCM measurement. (see Figure S2)

Once the feasibility of the LbL strategy is evidenced onto flat gold substrate, it was transposed to spherical templates, gold nanoparticles, having a well-defined size, dispersity and surface chemistry (sulfonated thiol stabilized gold nanoparticles) for the elaboration of capsules.

3.3.~~2.~~ From flat to colloidal gold substrates: Elaboration of cationic poly(cyclodextrin)-based nanocapsules

Zeta potential measurement is used herein to follow each stage of the polyelectrolyte deposition onto the spherical substrate (Figure 5 A). [23, 24] The ζ-potential values for pre-treated gold nanoparticles are -28 mV (± 2) due to the ionized sulfonate functions on the particle surface. As expected after the exposition of gold colloidal nanoparticles to $P(CD)^+$ and alginate solution, the value alternately switches to a positive one (~ +20 mV) and to a negative value (~ -20 mV), respectively. This clearly indicates the successful stepwise growth of polyelectrolytes multilayer films on colloids though robust adsorption of both polycationic and polyanionic polymers onto the colloidal material. [25-28]

We have evidenced the adsorption onto the gold nanoparticles surface by exploiting the sensitivity of the gold nanoparticle's surface Plasmon band.[13, 29] Towards this aim, UV-vis spectroscopy technique was used to follow each step of surface coating with the polyelectrolytes (Figure 5B). The absorption peak is correlated to the transverse surface Plasmon band of the bare colloidal gold nanoparticles. Compared to the bare gold nanoparticles, the coating of the gold nanoparticles with 2 and 4 $(P(CD^+)/alg^-)$ leads to a red-shift of 2 and 6 nm respectively in the Plasmon band maxima. All samples present stable electronic absorption spectra up to 4 weeks. The colloidal stability was also measured at 25°C and 37°C up to one month by DLS and zeta, a very good stability was observed, i.e. for $((P(CD^+)/alg^-)_4$ $P(CD^+)$ around 60 nm and -20 mV. Moreover, the absence of a Plasmon band blue-shift clearly demonstrated the robust deposition of the polyelectrolytes on the gold nanoparticles that is a crucial point for the elaboration of stable hollow nanoparticles.

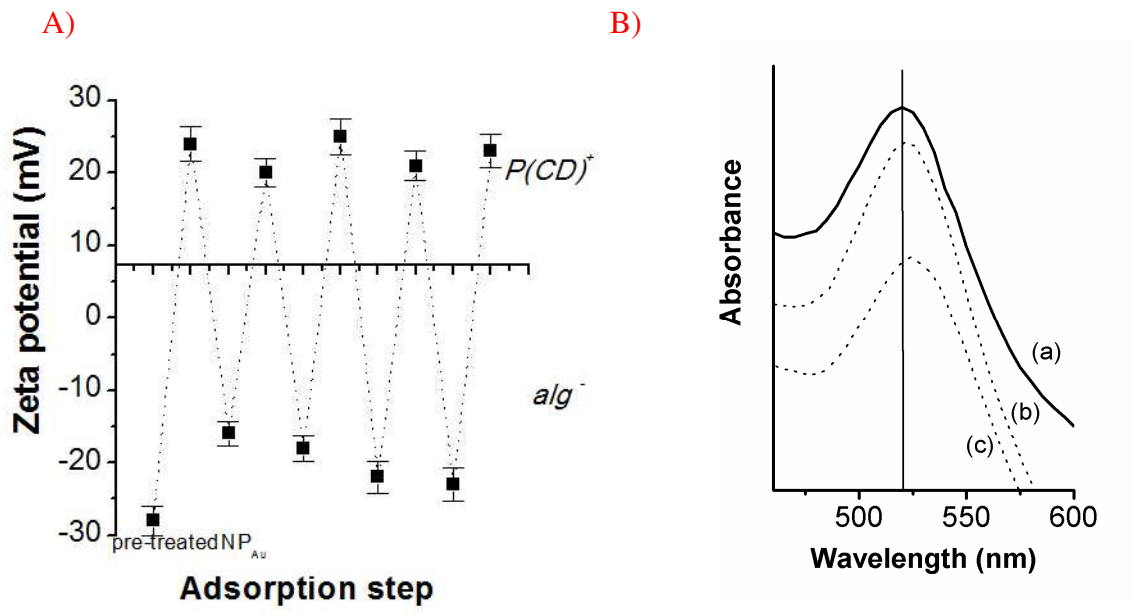

Figure 5: A) Zeta potential values measured upon alternating adsorption of P(CD$^+$) with alg$^-$ on pre-treated gold nanoparticles. B) UV-vis spectra of polyelectrolyte-coated gold nanoparticle as a function of the number of adsorbed polymer layers: curve a: uncoated gold nanoparticles; curve b: (P(CD$^+$)/alg$^-$)$_2$; curve c: (P(CD$^+$)/alg$^-$)$_4$; Curves are offset for clarity.

A major extension of core-shell particles technology is the removal of the core, leading to hollow particles (nanocapsules) that are replicas of the template-core. The procedure lies on the inherent permeability of the multilayer shell enabling diffusion-controlled removal of the core decomposition components. Sufficient shell permeability is required to preserve the structural integrity of the hollow particles. Herein, the removal of the gold cores and consequently the formation of nanocapsules were induced through cyanide etching of the gold core. This leads to the formation of gold cyanide complexes (4 Au + 8 KCN + 2 H_2O + O_2 → 4 KOH + 4 $KAu(CN)_2$) that can leach through the polymer capsule shell. This can be easily performed by repeated dialysis process.[30] The dissolution process of the gold core was monitored by the change in the UV/Vis spectrum. As evidenced from figure 6, a gradual disappearance of the absorbance peak is observed due to KCN treatment. This result is in accordance with the dissolution of the gold core by cyanide (Figure 6). No presence of atomic gold was detected by inductively coupled plasma optical emission spectrometry analysis in the last dialysate solution and in the (P(CD$^+$)/alg$^-$)$_n$ nanocapsules.

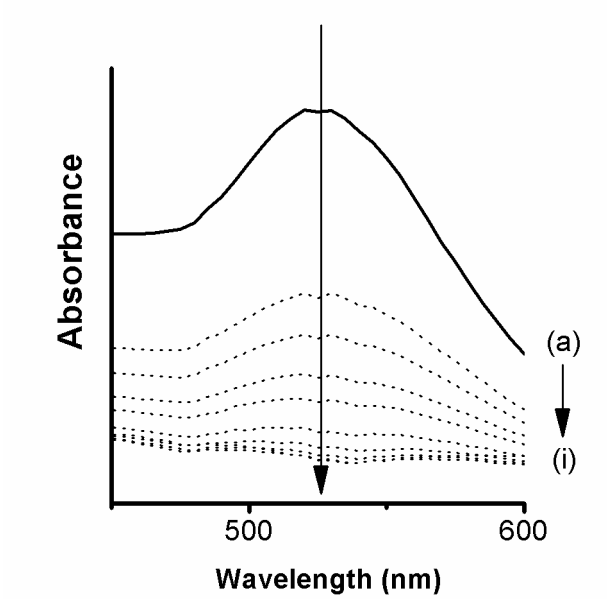

Figure 6: UV-vis spectra of $(P(CD^+)/alg^-)_4$ coated gold nanoparticle as a function of gold etching time: (a) 0 min, (b) 5 min, (c) 10 min, (d) 15 min, (e) 20 min, (f) 30 min, (g) 40 min, (h) 50 min and (i) 60 min.

Direct visualization of the morphology of bare gold nanoparticles, polymer-coated gold nanoparticles and nanocapsules is provided by TEM micrograph of air-dried polymer capsule (Figure 7). As observed, after core dissolution by treatment with an aqueous solution of KCN, we successfully obtain capsules (Figure 7C).

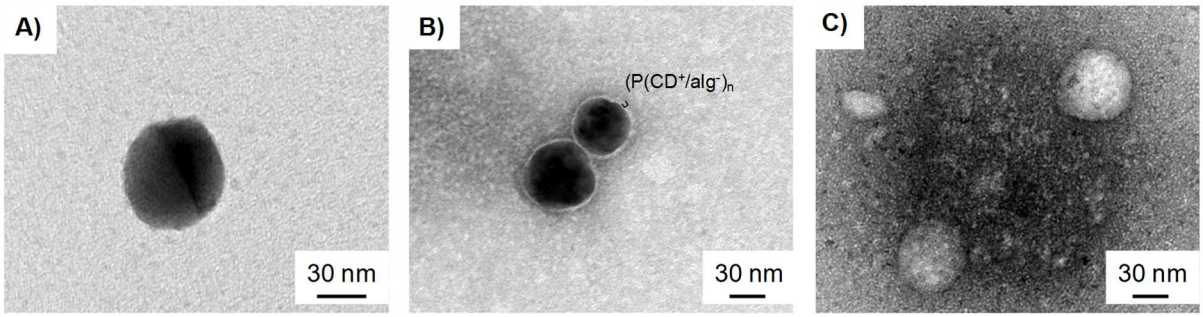

Figure 7: TEM micrographs of: A) bare gold nanoparticles, B) $(P(CD^+)/alg^-)_4$-coated gold nanoparticles and C) $(P(CD^+)/alg^-)_4$ nanocapsules.

Pyrene is a fluorescent probe whose emission spectrum changes in response to changes in polarity of the surrounding solvent.[31] The intensity ratio of the first peak (372 nm) and the third peak (382 nm) - I_{372}/I_{382} - in its fluorescent spectrum is classically used to evidence of a subtle environment change in terms of polarity. [32] For instance, the decrease in I_{372}/I_{382} intensity indicates the formation of hydrophobic clusters expected to occur with the aggregation of amphiphilic polymers. [33] At the studied pyrene concentration of 4.10^{-7}

mol.L^{-1}, no excimer band due to the interaction of an excited- and ground-state pyrene species was observed. [34-36] Such a low concentration was indeed chosen to minimize the influence of pyrene on the formation and/or the stability of hydrophobic domains. The initial I_{372}/I_{382} value of the pyrene solution at 4.10^{-7} mol.L^{-1} is found to be around 1.8 which is the classical value obtained for the pyrene in water at this concentration. After incubation with the P(CD^+), this value decreases to 0.8-0.9.

Of utmost importance, a similar I_{372}/I_{382} value of 0.8-0.9 is measured for the nanocapsules composed by pyrene-loaded P(CD^+) and alginate, and the ratio value is found to be independent of the number of multilayers from 2 to 4. As a control experiment, we prepared nanocapsules using chitosan as polycation instead of the cationic polycyclodextrin. Chitosan is a linear copolymer of β–(1,4)-2-amino-2-deoxy-D-glucose and N-acetyl-D-glucosamine in variable ratios that bears does positive charges in acidic conditions but does not provide hydrophobic interaction domains. Chitosan is not able to be implied in host-guest inclusion complex formation in contrast to CD-based polymers. In the case of the chitosan/alginate nanocapsules, the I_{372}/I_{382} value is measured around 1.8. This result can be fully explained by the fact that neither chitosan nor alginate can entrap pyrene through hydrophobic interaction and more importantly that the entrapment of pyrene within P(CD^+)/alginate results from host–guest complex formation. We quantified the amount of pyrene entrapped in the capsules by fluorescence intensity measurements. After extraction of pyrene from the CD cavity with methanol, the effective concentration of pyrene in 100 µL of a capsule suspension was found to be 0.145 and 0.310 µmol.L^{-1} for pyrene-loaded particles coated with $(P(CD^+)/alg^-)_n$-P(CD^+) with *n*= 2 and 4 respectively.

Then, a chemical presenting a biological activity, namely 4-hydroxy tamoxifen, has been loaded instead of pyrene. The ability of OHT-loaded $(PCD^+/alg^-)_2$-PCD^+ nanomaterials to be incorporated inside immortalized podocytes was investigated and the impact of the presence gold core was also studied. The OHT-loaded nanomaterials induce Cmip exon 8 deletion, deletion highlighted by specific PCR reaction. This technique leads to a 976 bp exon 8 floxed-arm band that is reduced or may fade out after deletion. In the conditions used for this experiment, exposure to the OHT-loaded nanovectors after 48h changes Cmip lox percentage. The quantification of the PCR bands is shown on Figure 8. Note that the hydroxy-tamoxifen-loaded nanomaterials have been dispersed in the culture medium. These nanoparticles could be used for cellular tests even after two months. The same biological results are obtained. This evidenced unambiguously the stability of the loaded nanoparticles in the culture medium.

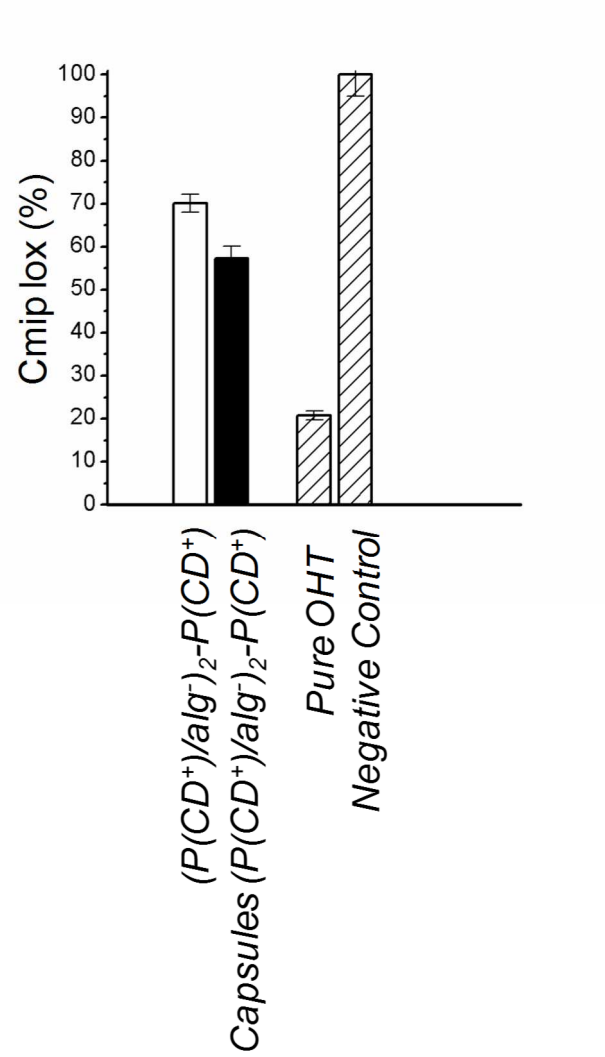

462

463 *Figure 8: Quantification of Cmip lox PCR products in each condition: (P(CD⁺)/alg⁻)₂-*
464 *P(CD⁺)-coated gold nanoparticles, (P(CD⁺)/alg⁻)₂-P(CD⁺) nanocapsules, OHT (positive*
465 *control) and negative control (cells, untreated with nanoparticles) characterizing the full*
466 *Cmip lox expression.*

467

468 A significant Cmip lox exon 8 band decrease (figure 8) can be observed after exposure to
469 nanomaterials for 48h, i.e. 70.1% for P(CD⁺)-coated nanoparticles with 2 layers. After
470 removing the gold core, this value is 57.2 % P(CD+)-nanocapsules with 2 layers respectively.
471 Note that with the 1 ~~µM~~ µmol.L^{-1} 4-hydroxdy-tamoxifen solution, the percentage falls below
472 20%. All these results are expressed in percentage of the negative control. This data suggests
473 that the nanomaterials are able to enter cells and that the 4-hydroxy tamoxifen retains its
474 biological activity despite encapsulation. While we expected that hollow nanocapsules would
475 be more malleable, more flexible compared to the coated gold nanoparticles, thus allowing a

better penetration into podocytes and, by extension, a greater Cmip extinction. Further experiments are required to understand the role of the structure and composition of nanoparticles as factors influencing the entry pathway and the molecule release.

In addition, a toxicity test (A morphological study by indirect *immunofluorescence* with Annexin V or cleaved caspase 3) could show higher mortality after exposure to gold nanoparticles (data not shown).

4. Conclusion

We demonstrate an easy and efficient approach combining both templating method, self-assembly and host–guest complexation to obtain well-designed and stable cyclodextrin-containing capsules in aqueous system. This elegant strategy requires neither surfactants nor even organic solvents. The elaboration of these capsules relies on the ability of cationic-poly(cyclodextrin) to be layer-by-layer assembled with alginate onto sacrificial particles. The built-up process is driven by electrostatic interactions in aqueous solution as evidenced by zeta measurements. The results of TEM and Au plasmon absorbance evidence the successful formation of nanocapsules with spherical shape. We gained advantage of the presence of CD cavities to entrap 4-hydroxy tamoxifen within the nanocapsules' shell through inclusion complexion formation. It was further shown that 4-hydroxy tamoxifen can be efficiently delivered to podocytes in vitro using CD-containing nanocapsules as carriers.

5. References

[1] A. Agarwal, Y. Lvov, R. Sawant, V. Torchilin, Stable nanocolloids of poorly soluble drugs with high drug content prepared using the combination of sonication and layer-by-layer technology, Journal of Controlled Release, 128 (2008) 255-260.

[2] R.C. Smith, M. Riollano, A. Leung, P.T. Hammond, Layer-by-Layer Platform Technology for Small-Molecule Delivery, Angewandte Chemie International Edition, 48 (2009) 8974-8977.

[3] S. Mura, J. Nicolas, P. Couvreur, Stimuli-responsive nanocarriers for drug delivery, Nat Mater, 12 (2013) 991-1003.

[4] Q.-D. Hu, G.-P. Tang, P.K. Chu, Cyclodextrin-Based Host–Guest Supramolecular Nanoparticles for Delivery: From Design to Applications, Accounts of Chemical Research, 47 (2014) 2017-2025.

[5] X. Yang, S. Johnson, J. Shi, T. Holesinger, B. Swanson, Polyelectrolyte and molecular host ion self-assembly to multilayer thin films: An approach to thin film chemical sensors, Sensors and Actuators B: Chemical, 45 (1997) 87-92.

[6] K. Sato, I. Suzuki, J.-i. Anzai, Preparation of Polyelectrolyte-Layered Assemblies Containing Cyclodextrin and Their Binding Properties, Langmuir, 19 (2003) 7406-7412.

[7] K. Sato, I. Suzuki, J.-i. Anzai, Layered assemblies composed of sulfonated cyclodextrin and poly(allylamine), Colloid and Polymer Science, 282 (2004) 287-290.

[8] I. Suzuki, Y. Egawa, Y. Mizukawa, T. Hoshi, J.-i. Anzai, Construction of positively-charged layered assemblies assisted by cyclodextrin complexation, Chemical Communications, (2002) 164-165.
[9] A. Van der Heyden, M. Wilczewski, P. Labbe, R. Auzely, Multilayer films based on host-guest interactions between biocompatible polymers, Chemical Communications, (2006) 3220-3222.
[10] O. Kaftan, S. Tumbiolo, F. Dubreuil, R. Auzély-Velty, A. Fery, G. Papastavrou, Probing Multivalent Host–Guest Interactions between Modified Polymer Layers by Direct Force Measurement, The Journal of Physical Chemistry B, 115 (2011) 7726-7735.
[11] G.V. Dubacheva, P. Dumy, R. Auzely, P. Schaaf, F. Boulmedais, L. Jierry, L. Coche-Guerente, P. Labbe, Unlimited growth of host-guest multilayer films based on functionalized neutral polymers, Soft Matter, 6 (2010) 3747-3750.
[12] L.L. del Mercato, M.M. Ferraro, F. Baldassarre, S. Mancarella, V. Greco, R. Rinaldi, S. Leporatti, Biological applications of LbL multilayer capsules: from drug delivery to sensing, Adv Colloid Interface Sci, 207 (2014) 139-154.
[13] S. Belbekhouche, O. Mansour, B. Carbonnier, Promising sub-100 nm tailor made hollow chitosan/poly (acrylic acid) nanocapsules for antibiotic therapy, Journal of colloid and interface science, 522 (2018) 183-190.
[14] N. Thuaud, B. Sebille, A. Deratani, G. Lelievre, Retention behavior and chiral recognition of β-cyclodextrinderivative polymer adsorbed on silica for warfarin, structurally related compounds and Dns-amino acids, Journal of Chromatography A, 555 (1991) 53-64.
[15] A.K. Indra, X. Warot, J. Brocard, J.-M. Bornert, J.-H. Xiao, P. Chambon, D. Metzger, Temporally-controlled site-specific mutagenesis in the basal layer of the epidermis: comparison of the recombinase activity of the tamoxifen-inducible Cre-ERT and Cre-ERT2 recombinases, Nucleic acids research, 27 (1999) 4324-4327.
[16] R. Feil, J. Brocard, B. Mascrez, M. LeMeur, D. Metzger, P. Chambon, Ligand-activated site-specific recombination in mice, Proceedings of the National Academy of Sciences of the United States of America, 93 (1996) 10887-10890.
[17] A. Moktefi, S.Y. Zhang, P. Vachin, V. Ory, C. Henique, V. Audard, C. Rucker-Martin, E. Gouadon, M. Eccles, A. Schedl, L. Heidet, M. Ollero, D. Sahali, A. Pawlak, Repression of CMIP transcription by WT1 is relevant to podocyte health, Kidney international, 90 (2016) 1298-1311.
[18] E. Memisoglu-Bilensoy, I. Vural, A. Bochot, J.M. Renoir, D. Duchene, A.A. Hıncal, Tamoxifen citrate loaded amphiphilic β-cyclodextrin nanoparticles: In vitro characterization and cytotoxicity, Journal of Controlled Release, 104 (2005) 489-496.
[19] S. Daoud-Mahammed, P. Couvreur, K. Bouchemal, M. Chéron, G. Lebas, C. Amiel, R. Gref, Cyclodextrin and Polysaccharide-Based Nanogels: Entrapment of Two Hydrophobic Molecules, Benzophenone and Tamoxifen, Biomacromolecules, 10 (2009) 547-554.
[20] E. Renard, A. Deratani, G. Volet, B. Sebille, Preparation and characterization of water soluble high molecular weight β-cyclodextrin-epichlorohydrin polymers, European Polymer Journal, 33 (1997) 49-57.
[21] I. Colinet, V. Dulong, T. Hamaide, D. Le Cerf, L. Picton, New amphiphilic modified polysaccharides with original solution behaviour in salt media, Carbohydrate Polymers, 75 (2009) 454-462.
[22] K. Kalyanasundaram, J.K. Thomas, Environmental effects on vibronic band intensities in pyrene monomer fluorescence and their application in studies of micellar systems, Journal of the American Chemical Society, 99 (1977) 2039-2044.
[23] S.E. Burke, C.J. Barrett, pH-Responsive Properties of Multilayered Poly(l-lysine)/Hyaluronic Acid Surfaces, Biomacromolecules, 4 (2003) 1773-1783.

[24] S. Belbekhouche, S. Charabi, S. Hamadi, B. Carbonnier, Latex nanoparticles surface modified via the layer-by-layer technique for two drugs loading, Colloids and Surfaces A: Physicochemical and Engineering Aspects, 524 (2017) 28-34.
[25] F. Caruso, H. Lichtenfeld, E. Donath, H. Möhwald, Investigation of Electrostatic Interactions in Polyelectrolyte Multilayer Films: Binding of Anionic Fluorescent Probes to Layers Assembled onto Colloids, Macromolecules, 32 (1999) 2317-2328.
[26] F. Caruso, R.A. Caruso, H. Möhwald, Nanoengineering of inorganic and hybrid hollow spheres by colloidal templating, Science, 282 (1998) 1111-1114.
[27] F. Caruso, Hollow capsule processing through colloidal templating and self-assembly, Chemistry-A European Journal, 6 (2000) 413-419.
[28] G. Sukhorukov, A. Fery, H. Möhwald, Intelligent micro- and nanocapsules, Progress in Polymer Science, 30 (2005) 885-897.
[29] D.I. Gittins, F. Caruso, Multilayered polymer nanocapsules derived from gold nanoparticle templates, Advanced Materials, 12 (2000) 1947-1949.
[30] D.I. Gittins, F. Caruso, Tailoring the polyelectrolyte coating of metal nanoparticles, The Journal of Physical Chemistry B, 105 (2001) 6846-6852.
[31] Z. Liu, J. Ou, H. Lin, H. Wang, J. Dong, H. Zou, Preparation of polyhedral oligomeric silsesquioxane-based hybrid monolith by ring-opening polymerization and post-functionalization via thiol-ene click reaction, Journal of Chromatography A, 1342 (2014) 70-77.
[32] E.D. Goddard, N.J. Turro, P.L. Kuo, K.P. Ananthapadmanabhan, Fluorescence probes for critical micelle concentration determination, Langmuir, 1 (1985) 352-355.
[33] W. Henni, M. Deyme, M. Stchakovsky, D. LeCerf, L. Picton, V. Rosilio, Aggregation of hydrophobically modified polysaccharides in solution and at the air-water interface, J Colloid Interface Sci, 281 (2005) 316-324.
[34] M.M. Amiji, Pyrene fluorescence study of chitosan self-association in aqueous solution, Carbohydrate Polymers, 26 (1995) 211-213.
[35] A. Fischer, M.C. Houzelle, P. Hubert, M.A.V. Axelos, C. Geoffroy-Chapotot, M.C. Carré, M.L. Viriot, E. Dellacherie, Detection of Intramolecular Associations in Hydrophobically Modified Pectin Derivatives Using Fluorescent Probes, Langmuir, 14 (1998) 4482-4488.
[36] S. Belbekhouche, J. Desbrières, T. Hamaide, D. Le Cerf, L. Picton, Association states of multisensitive smart polysaccharide–block-polyetheramine copolymers, Carbohydrate Polymers, 95 (2013) 41-49.

613 **Supporting information**
614

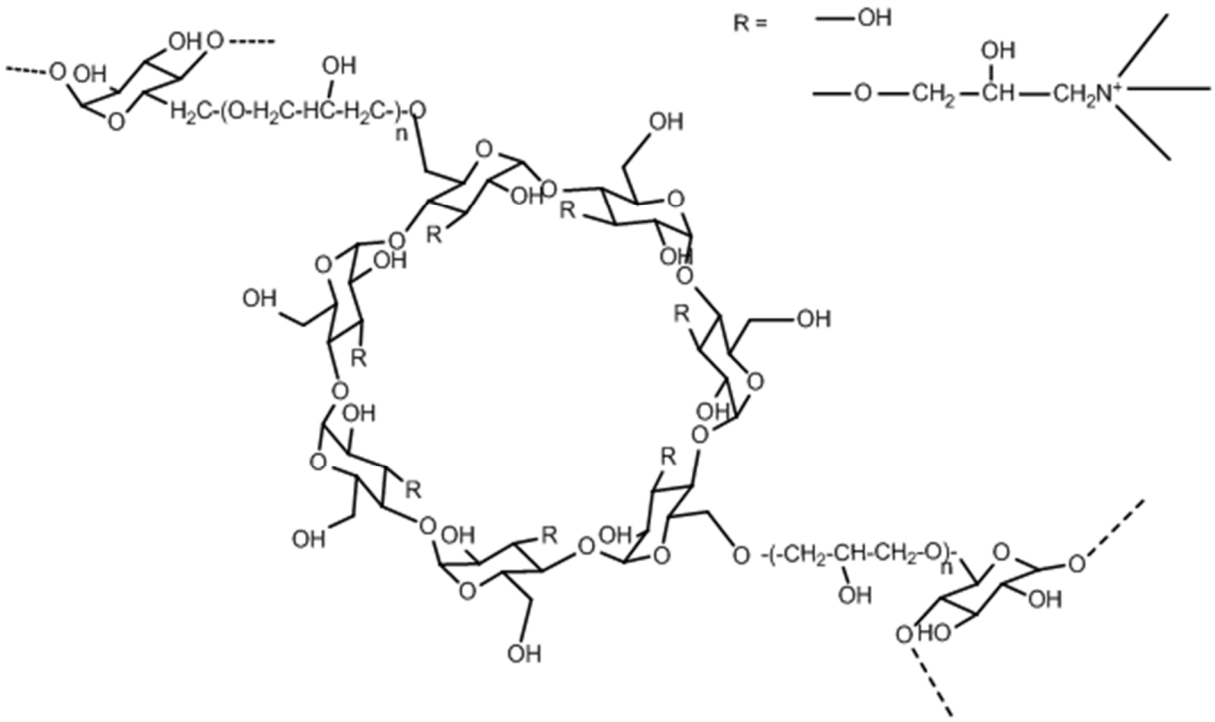

615
616 Figure S1: Proposed structure of cationic poly(β-cyclodextrin)
617
618
619

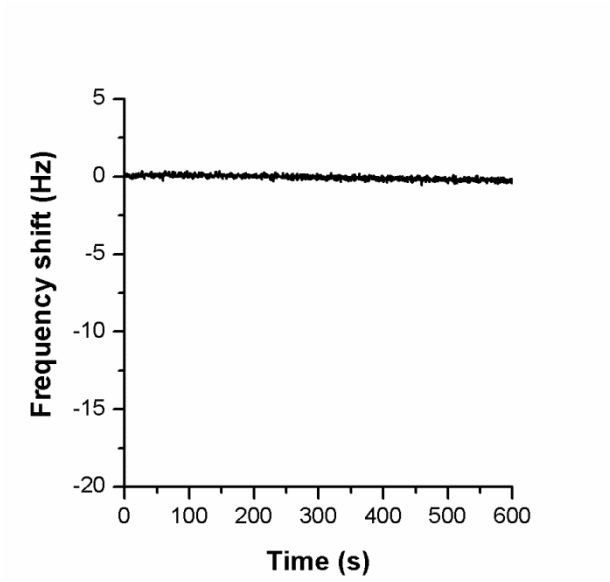

620
621 **Figure S2**: QCM-D measurements. Flushing of a gold sensor coated with $(P(CD^+)/alg^-)_4$
622 $P(CD^+)$ film with the culture medium. The non variation of the frequency evidences the
623 stability of the multilayer films under such condition.

Graphical Abstract